The Role of N$_2$ as booter gas during Enhanced Gas Recovery by CO$_2$ flooding in porous medium

Nuhu Mohammed*, Abubakar J. Abbas, Godpower C. Enyi.

*Corresponding author: (n.mohammed5@edu.salford.ac.uk)

Abstract

Most research on CO$_2$ flooding is focusing on CO$_2$ storage than CH$_4$ recovery and mostly simulation-based. To our knowledge, there have been limited reported experimental on CO$_2$ injections capable of unlocking a high amount of the residual methane due to their miscibility effect. The empirical study has highlighted the impact of N$_2$ as a booster gas during the Enhanced Gas Recovery (EGR) process by CO$_2$ flooding. The N$_2$ acts as a booster by re-pressurising the reservoir pressure before the CO$_2$ breakthrough, enabling more CH$_4$ recovery. It also acts as a retardant by creating a thin barrier at the CO$_2$-CH$_4$ interface, making it difficult for the CO$_2$ to disperse into the CH$_4$. This result in an extendable breakthrough, influencing the injected CO$_2$ to migrate downward due to gravity for storage within the pore spaces. This study, a core flooding experiment at 1500 psig and 40 ^{0}C of pressure and temperature, respectively, was carried out to study the effect of N$_2$ as booster gas during natural displacement in a porous medium (sandstone rock). The recoveries with N$_2$ booster were better off than those without N$_2$ booster (conventional CO$_2$ flooding). Overall, an improved CH$_4$ recovery and dispersion coefficient with substantial storage was noticed, with the optimum at 0.13 fraction of pore volume booster gas. Compared to the 0.4ml/min optimum conventional CO$_2$ injection, the results show a 10.64 and 24.84% increase in CH$_4$ recovery and CO$_2$ storage, respectively. 0.71 x 10-8 m^2/s reduction in dispersion coefficient was recorded than the convention method. The additional CH$_4$ recovery can provide extra revenue to offsets other operational expenses. This research signifies the potential of N$_2$ as a booster medium on CH$_4$ recovery, which can be applicable for pilot application within the oil and gas industry.

Keywords: Dispersion coefficient; CO$_2$ storage; CO$_2$-breakthrough, booster, methane displacement

1. Introduction

The method of injecting CO$_2$ to recover residual natural gas is gaining recognition within the oil and gas industry. A substantial injected volume of CO$_2$ stored provides an additional advantage over the conventional Carbon Capture and Storage (CCS) process. The natural gas recovered can provide extra revenue to offset other operational costs. This mechanism involving a tertiary recovery method is called Enhanced Gas Recovery (EGR) process. Since both CO$_2$ and CH$_4$ are gases, their properties were potentially agreeable for reservoir application due to unique behaviour, and phase change demonstrates by CO$_2$ at supercritical conditions (Oldenburg and Benson, 2002). The density ratio of CO$_2$ to CH$_4$ is in the range of 2–6 at reservoir states (Al-Hasami et al., 2005), which make CO$_2$ to be classified as high viscous gas (Al-Hasami et al., 2005). Thus, CO$_2$ can be migrated downwards for storage during the EGR process (Oldenburg et al., 2001). More so, CO$_2$ is more soluble in formation water than CH$_4$ due to its high solubility factor in aqueous solvents. The EGR process is a promising technique for co-current CH$_4$ gas recovery and CO$_2$ storage during natural displacement in a porous medium. However, CO$_2$ and CH$_4$ are completely miscible due to the similarities in their physical properties. This result in an early CO$_2$ breakthrough during the natural gas displacement process, which has been the major drawback of the technology (Li et al., 2019; Oldenburg & Benson, 2002; Shtepani, 2006; Turta et al., 2007; Sim et al., 2008; Al-abri et al., 2009; S. Sim et al., 2009; Sidiq et al., 2011; Hughes et al., 2012; Honari et al., 2013; Khan et al., 2013; Zhang et al., 2014; Honari et al., 2015; Patel et al., 2016; Honari et al., 2016). This problem has affected its applicability within the oil and gas industry because of product contamination because of the high amount of CO$_2$ recorded at the outlet stream (Oldenburg & Benson 2002; S. S. K. Sim et al., 2009).

Abba et al. (2018) investigated the impact of connate water salinity on the dispersion coefficient in consolidated rocks during the EGR process by CO$_2$ flooding. The experiment was carried out at 50 ^{0}C and 1300 psig of temperature and pressure, respectively. The optimum CO$_2$ injection occurred at 0.3ml/min, and their result from the core flooding process indicated that the dispersion coefficient decreases with increasing salinity. Hence, the higher the density of the

connate water, the lower the dispersion of CO_2 into CH_4. They use varying salinity concentration, and they were able to report 20 minutes extendable CO_2 breakthrough at a maximum concentration of 10 % wt. sodium chloride (NaCl). Unfortunately, a decline in CH_4 recovery was recorded as the salt concentration increases from 5-10 %wt., due to the reduction in core sample pore volume causes by the high-density connate water molecule occupying more of the free bubble holes within the core matrix (Abba et al., 2019).

To our knowledge, there are limited experimental findings on CO_2 injections capable of unlocking the residual natural gas with a substantial volume of injected CO_2 stored due to their miscibility effect (Abba et al., 2018). This necessitated the need for an in-depth study of using N_2 as a booster before CO_2 introduction. In so doing, the nascent mixing between the two gases (CO_2 and CH_4) is minimized since injecting a specific volume of N_2 prior to the CO_2 injection exhibits a re-pressurization effect that yields more CH_4 recovery and a minimum fraction of CO_2 in the effluent stream of the core holder before and after the CO_2 breakthrough. It was evident from the gas chromatography (GC) print out, which results in delaying the CO_2 gaining access to the CH_4 boundary, making the process more efficient since less product contamination was recorded than the conventional CO_2 flooding. More so, determining the best CO_2 injection rate before the N_2 booster gas inclusion its prerequisite for optimum booster gas volume needed to provide maximum CH_4 recovery and minimum CH_4-CO_2 miscibility (dispersion coefficient).

This paper's objective highlighted the role of N_2 as a booster for CH_4 recovery during the EGR process by CO_2 flooding. The N_2 gas acts as a booster, enabling more CH_4 recovery without cross-contamination, making it difficult for the CO_2 to disperse into CH_4, resulting in a longer CO_2-breakthrough due to the N_2 blanketing effect. This makes the CO_2 descend downward for storage within the pore spaces due to gravity. In this paper, the impact of N_2 as booster gas for natural gas recovery enhancement and miscibility reduction during the CO_2 flooding displacement process was investigated. The experimental runs with N_2 as booster show a promising recovery and CO_2 storage with less contamination than those without a booster gas (conventional CO_2 flooding).

2. Overview Concepts and Theories

The conventional or traditional approach for CH_4 recovery by CO_2 injection is depletion development, but such recovery (approximately 35 %) is deemed low to offset the CO_2 storage cost (Wang et al., 2018). Due to the nascent mixing between the injected CO_2 and displaced CH_4, an invariable amount to premature CO_2 breakthrough in the production well. The aim was to recover a substantial CH_4 free from CO_2, enabling more injected CO_2 stored in the process. However, that was difficult using the conventional EGR-CO_2 injection technique. High injected CO_2 fraction was noticed early before or after breakthrough, as seen in Fig. 1, and the value of X_0 at the intersection point (1) in Fig. 3. Therefore, a new EGR approach is required to reduce the mole fraction of CO_2 in the recovered CH_4. The N_2 gas act as a booster by re-pressurising the reservoir pressure before CO_2 breakthrough enable more CH_4 recovery without contamination. It also acts as a retardant by creating a thin barrier between the CO_2-CH_4 phase region presented in Fig. 2. This makes it difficult for the CO_2 to disperse into CH_4, resulting in a longer CO_2 breakthrough, making most of the injected CO_2 descending downward for storage within the pore spaces due to gravity. In this study, N_2 was employed as a booster gas to delayed CO_2 breakthrough with minimum miscibility. In the process, more CH_4 recovery and CO_2 storage were realised, since the produced CO_2 fraction has reduced as shown from intersection points (2) and (3), X_1, and X_2 in Fig. 3. To maximise both CH_4 recovery and CO_2 storage; (1) the fraction of the produced CO_2 (X_0, X_1, and X_2) needs to be minimised ($X_2 < X_1 < X_0$), (2) the change in the produced CO_2 fraction (ΔX) and slope (S_1 and S_2) also have to be maximised ($\Delta X_2 > \Delta X_2$ and $S_2 > S_1$). Fig. 3 is the plot of produced CO_2 fractions against displaced CH_4 at 0.4ml/min optimum conventional CO_2 injection, 1500 psig of pressure, and 40 ^{0}C of temperature. These mole fractions are the effluent stream compositions recorded by the GC machine. The optimum booster gas volume was selected based on the above criteria.
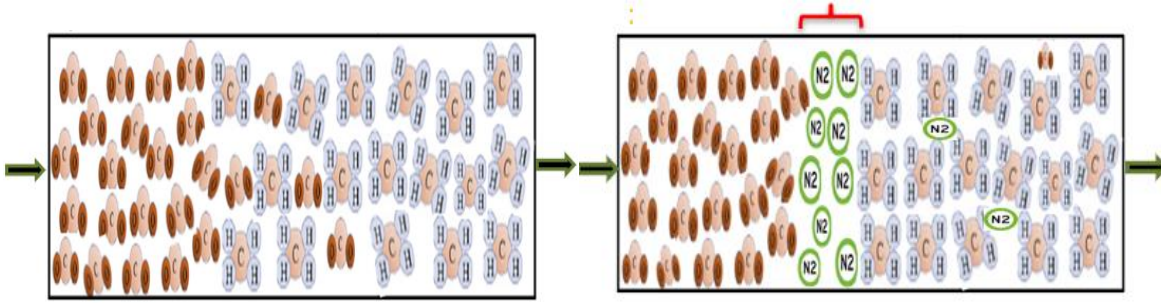
Fig. 1. Schematics of conventional CO_2 injection to displace CH_4 without N_2 booter gas (Wang et al., 2018)

Fig. 2. Schematics of conventional CO_2 injection to displace CH_4 with N_2 booster gas (Wang et al., 2018)
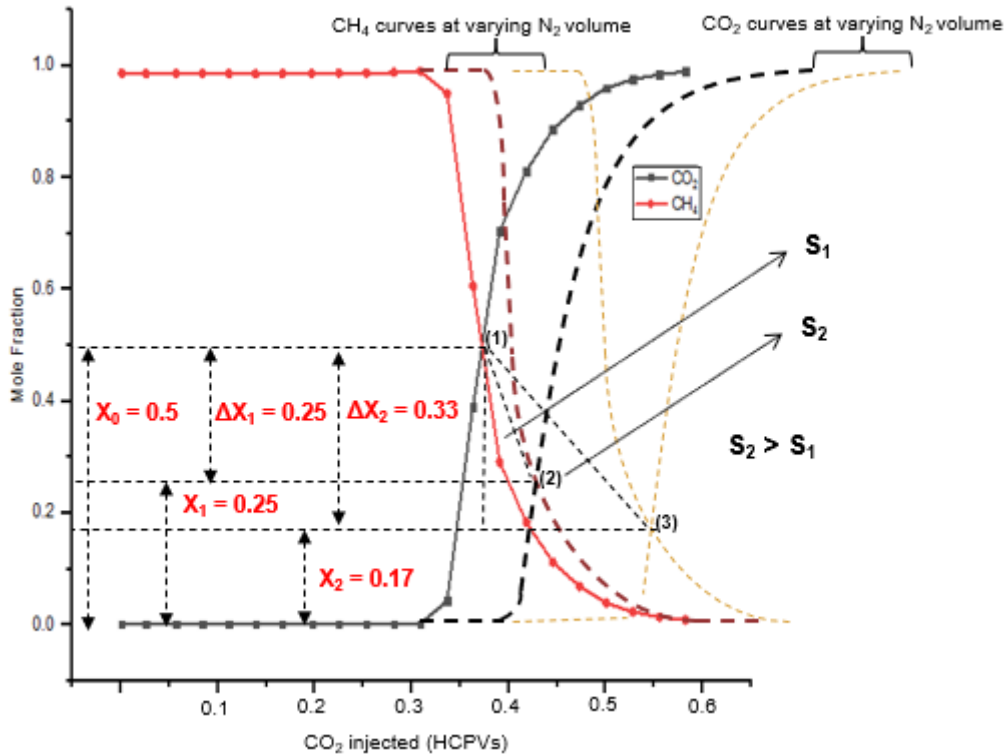

Fig. 3. Conventional CO_2 injection concentration profile for systematic optimisation purpose at 0.4ml/min, 1500 psig, and 40 °C (Mohammed et al., 2020).

2.1 Dispersion Coefficient

In this study, the fundamental model equations used are those developed and reported by (Newberg & Foh, 1988; Perkins & Johnston, 1963; Coats et al., 2009; Honari et al., 2013; Hughes et al., 2012; Mamora and Seo, 2002; Liu et al., 2015; Takahashi & Iwasaki, 1970; Abba et al., 2017; Abba et al., 2018; Abba et al., 2019; Fuller et al., 1966) as presented in Eqns. 1-9. Details of these equations can be found in our previous publications (Mohammed et al., 2019; Mohammed et al., 2020).

$$K_L \frac{\partial^2 C}{\partial x^2} - u \frac{\partial C}{\partial x} = \frac{\partial C}{\partial t} \tag{1}$$

Eqn. 1 describes the displacement of methane by carbon dioxide in consolidated rocks, where (C), (x), (u), and (K_L) are the effluent composition measured by the gas chromatography, distance under time (t), interstitial velocity, and longitudinal dispersion coefficient respectively. Invariably Eqn.1 can be re-written in a dimensionless form (Mamora and Seo, 2002), as shown in Eqn. 2.

$$\frac{1}{P_e}\frac{\partial^2 C}{\partial x_D^2} - \frac{\partial C}{\partial x_D} = \frac{\partial C}{\partial t_D} \qquad (2)$$

Where,

Parameter	Symbol	Expression
Peclet number	P_e	$\frac{uL}{K_L}$
Dimensionless time	t_D	$\frac{tu}{L}$
Dimensionless distance	x_D	$\frac{x}{L}$
Interstitial velocity	u	$\frac{Q}{\pi r^2 \phi}$

Since the injection of CO_2 is at x = 0, then

Initial condition: C = 0 at t_D = 0,

Boundary conditions: C = 1 at x_D = 0, C → 0 as x_D → ∞

Therefore, the solution to Eqn.2 is presented in Eq. 3.

$$C = \frac{1}{2}\left\{ erfc\left(\frac{x_D - t_D}{2\sqrt{t_D/P_{em}}}\right) + e^{P_{em}x_D} erfc\left(\frac{x_D + t_D}{2\sqrt{t_D/P_{em}}}\right)\right\} \qquad (3)$$

The effluent core flooding composition was fitted with the analytical solution to the one-differential Advection Dispersion (AD) equation (Eqn.3) in terms of the *Péclet* number to evaluate the corresponding dispersion coefficient. The experiment's absolute dispersion coefficient is the value that provides the optimum synergy between the experimental result compared to the numerical solution. The medium peclet number (P_{em}) shown in Eqn. 4 was used to predict the dominant displacement mechanism during the EGR process in a porous medium (Perkins & Johnston, 1963). The characteristic length scale (d) is in meters, while (D) represent the molecular diffusion coefficient in m²/s.

$$P_{em} = \frac{u_m d}{D} \qquad (4)$$

Generally, at P_{em} <0.1, diffusion dominates the dispersion process, and at P_{em}>10, advective mixing dominates the dispersion process (Perkins and Johnson, 1963). However, the process is under the intermediate zone when the *Péclet* number is greater than 0.1 but less than 10. The solution of Eqn.3 was used to fit the concentration profiles which the dispersion coefficient was then evaluated. Coats et al. (2009) correlated the dispersion coefficient with the molecular diffusion coefficient, as shown in Eq. 5

$$\frac{K_l}{D} = \frac{1}{\tau} + \alpha\frac{u_m^n}{D} \qquad (5)$$

Here α is the dispersivity of the porous medium (m), and (n) represents an exponent. The tortuosity (τ) ranges from 1 to as high as 13 or more for consolidated rocks, as reported by Honari et al. (2013). The parameter (τ) can be obtained empirically through various methods; however, α and n are mainly determined using a core flooding system (Hughes et al., 2012). The intercept from Eq.5 was used to calculate the tortuosity.

2.2 Diffusion Coefficient

The Takahashi & Iwasaki developed in 1970 has been used successfully for diffusion coefficient determination. However, it's mainly applied to the CO_2-CH_4 system only.   In this report, due to N_2 inclusion, a different model proposed by Fuller et al. (1966) was employed. This correlation presented in Eqn. 6 is applicable for both CO_2, N_2 and CH_4 system.

$$D_{\text{N2,CH4}} = \frac{1.0110 \times 10^{-4} \, T^{1.75} \sqrt{(1/\mu_{N_2} + 1/\mu_{CH_4})}}{P[(\Sigma V_{N_2})^{1/3} + (\Sigma V_{CH_4})^{1/3}]^2} \tag{6}$$

Where $(\Sigma \ V_{N_2})$ and $(\Sigma \ V_{CH_4})$ are the values derived from the summation of atomic diffusion volumes of N_2 and CH_4 molecules, respectively. These values are reported in our previous publications (Mohammed et al., 2019). The equation was further simplified to formed Eqns. 7 and 8 after inserting the values of atomic diffusion volumes and the molecular weight of N_2, CH_4 and CO_2.

$$D_{\text{N2,CH4}} = \frac{10.2 \times 10^{-11} \, T^{1.75}}{P} \tag{7}$$

$$D_{\text{CO2,CH4}} = \frac{8.2 \times 10^{-11} \, T^{1.75}}{P} \tag{8}$$

Where, T is the temperature in kelvin (K) and P is the pressure in megapascal (MPa).

3. Materials and Methods

In this study, the potential of N_2 for CH_4 recovery and CO_2 storage was investigated using the CO_2 flooding technique. This entails saturating the core plug with CH_4 at known irreducible water of saturation (Swi), injecting varying amounts of N_2 as a booster prior to CO_2 injection at an optimum rate of 0.4 ml/min. The property of the core plug employed was presented in Table 1.

Table 1. Specification and property of the Bandera grey core sample at experimental conditions

Core sample	Length (mm)	Diameter (mm)	Porosity (%)	Gas Permeability (mD)
Bandera gray	76.02	25.31	19.68	32

Procedure

The core sample was dried overnight in an oven at 105 ^{0}C for moisture removal and other volatile compounds. The dried sample was wrapped with cling film and foil paper before being inserted into a heat shrink. This is vital to avoid leaving viscous fingerprints and penetrating the gases through the sleeve into the ring-shaped core holder. The sample was loaded into the core holder and stapled with clamps from both ends. Hydraulic oil was pumped into the ring-shaped core holder to provide the desired overburden pressure, kept at a minimum of 500 psig above the pore pressures to avoid fracturing the core sleeve. The heat jacket was installed on the core holder, and the temperature step-up (40 ^{0}C) was observed before CH_4 saturation. The backpressure was engaged, the core sample was saturated with CH_4 at 10 % irreducible water saturation until the GC constantly read methane composition greater than 98 %. CO_2 was injected at 0.2 ml/min using ISCO pumps C/D through cell B. The experiment ended when the methane concentration was insignificant from the GC reading (when the mole fraction of produced CO_2 is > 98%). Further runs were carried out at increasing CO_2 injection rates of 0.4, 0.6, 0.8, and 1.0 ml/min. At each GC's injection time, the time was noted, and the effluent composition was recorded. The best injection rate was selected and employed as the next step of the experiment (with N_2 as booster gas). The sample was recleaned, dried, and re-saturated with CH_4. Following this, 0.06 HCPV of N_2 was then injected using ISCO pumps A/B through cell A. Further runs were carried out at increasing N_2 booster gas volumes. The experiment was carried out at relevant reservoir pressure of 1500 psig and 40 ^{0}C temperature.
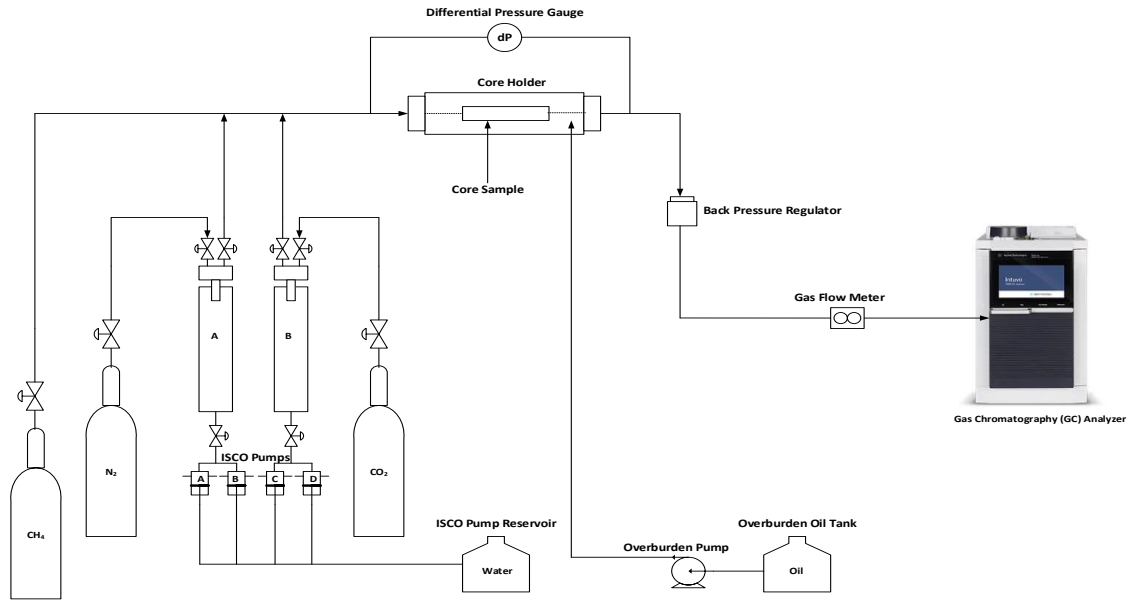
Fig. 4. Schematics of methane displacement with and without cushion gas

4. Results

4.1 Effect of CO_2 injections on Methane recovery

To evaluate the CH_4 recovery efficiency of each injection rate based on the gas production recorded, the Original Gas in Place (OGIP) was determined using Eqn.10. The porosity obtained from the Helium Porosimetry, the gas formation volume factor was evaluated at experimental conditions with the compressibility factor (Z), obtained numerically from models in the works reported by (Shabani and Vilcaez, 2017; Ziabakhsh-Ganji and Kooi, 2012). The CH_4 gas production was recorded online using the gas flow meter, and its composition was analysed regularly (at 5 minutes sequence) via the GC machine. The displacing gas migration and breakthroughs were observed in real-time, and the dispersion coefficient, recovery swept efficiency, and CO_2 storage was evaluated. The experiment stopped when the CO_2 produced was far more than its injected amount (the produced gas contained an insignificant amount of CH_4). The experimental results for the CO_2 produced at different injections (0.2-1.0 ml/min) were presented in Fig. 17. The miscible displacement takes place at the front of supercritical CO_2 (ScCO_2). The CO_2 injection up to 0.21 HCPV results in less CO_2 concentration at the outlet, insignificance natural gas contamination. In the process, the initial CH_4 recovery increased linearly. When 0.22 HCPV were injected, the composition of CO_2 in the effluent stream raised to about 5 %, invariable the percentage recovery increased by 3% to its peak value of 35 %. The point can be deemed as a breakthrough point. For injections after breakthrough, a sharp increase in the CO_2 outlet composition was noticed until 0.3 HCPV of CO_2 were injected, resulting in a high CH_4 recovery decline. Further injections to 0.372 HCPV showed less effect with both fractions of CO_2 produced and CH_4 recovery efficiency kept almost unchanged. This indicates the displacement has reached an endpoint. The same graph pattern was observed at 0.2ml/min injection. However, the CO_2 presence in the exit stream occurred earlier than that for 0.4ml/min, while its maximum CH_4 recovery was recorded when a total of 0.3 HCPV of CO_2 was injected into the system. This can be seen in Figs. 5 and 17, respectively. A similar trend was noticed in other injection rates, but the decline in methane recovery was huge at higher injection rates (0.6-1.0 ml/min) with an average of 20 % decline, as seen in Fig. 17. More so, the breakthrough graphs at higher injection rates (0.6-1.0ml/min) in Figs. 7, 8, and 9 showcase high slope due to the curves' stiffness after the CO_2 breakthrough. This signifies the possibility of high miscibility between the CO_2 and CH_4 during the displacement process. Overall, there was a substantial methane recovery at lower injection rates (0.2-0.4ml/min) than those at high injections (0.6-1.0 ml/min). At

these rates, poor recovery and sweep efficiency were observed due to higher interstitial velocity. Abba et al. (2018) reported a high interstitial velocity tends to increase the turbulence and eddy current of the flow profile and agitate the gas species' molecules, facilitating the interaction collision between the displacing and displaced gases. This results in a high dispersion coefficient, as seen in Table 2.
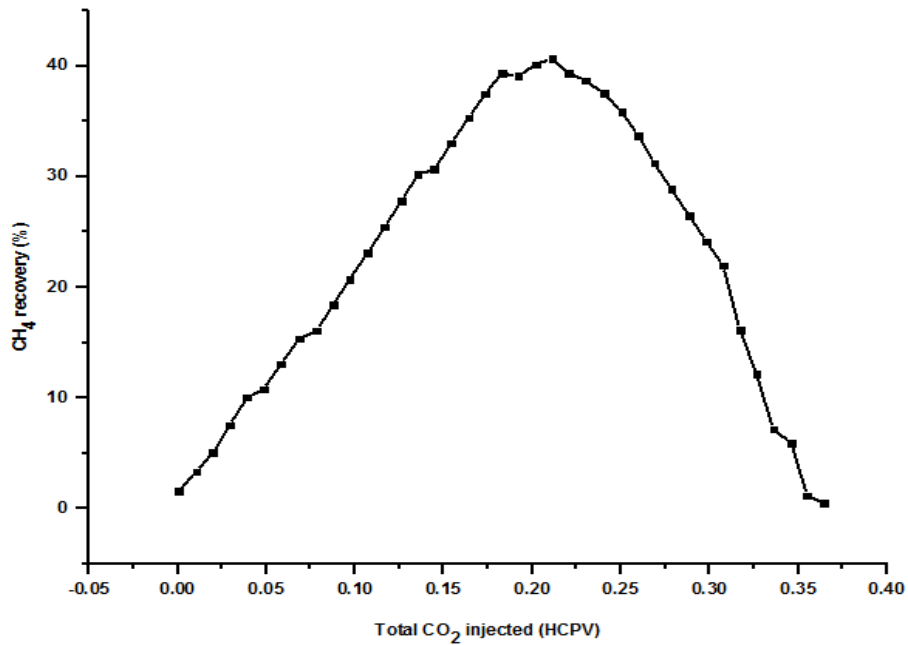
$$OGIP = \frac{V_b \phi (1 - s_{wi})}{B_g} \qquad (10)$$

Fig. 5. CH_4 recovery against HCPV of total CO_2 injected at 0.2ml
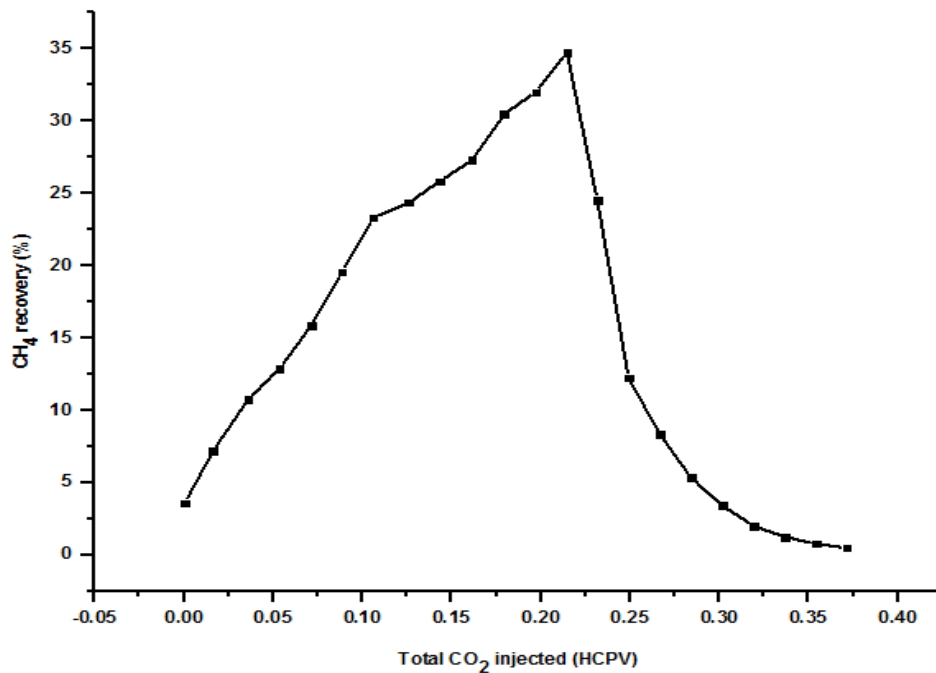
Fig. 6. CH_4 recovery against HCPV of total CO_2 injected at 0.4ml
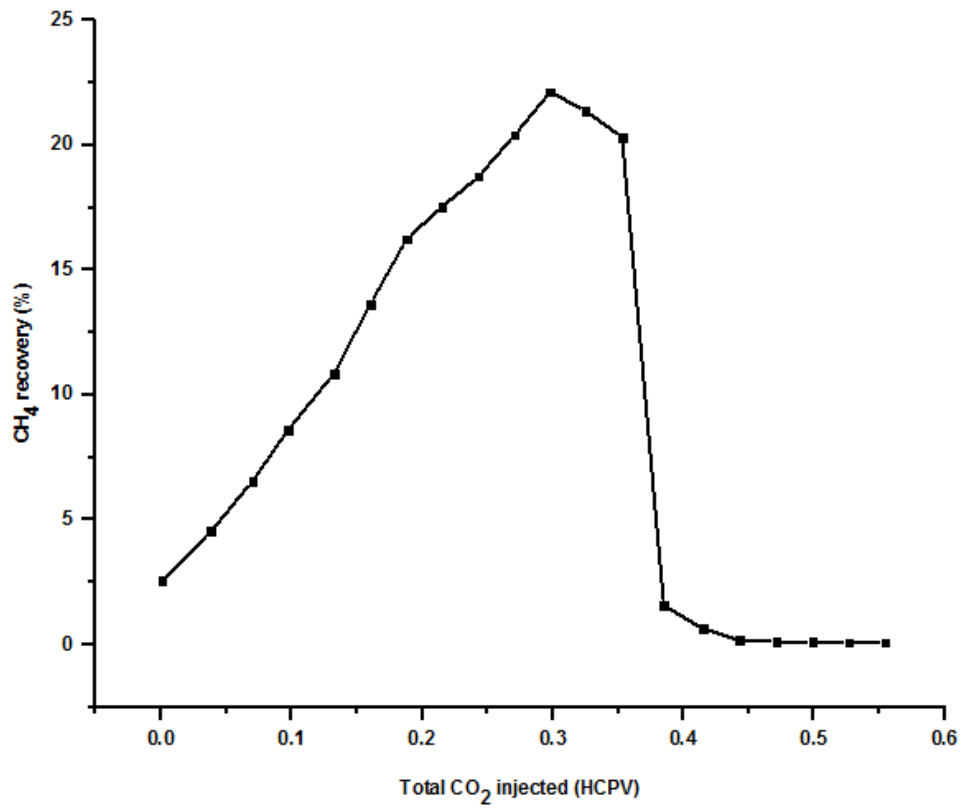
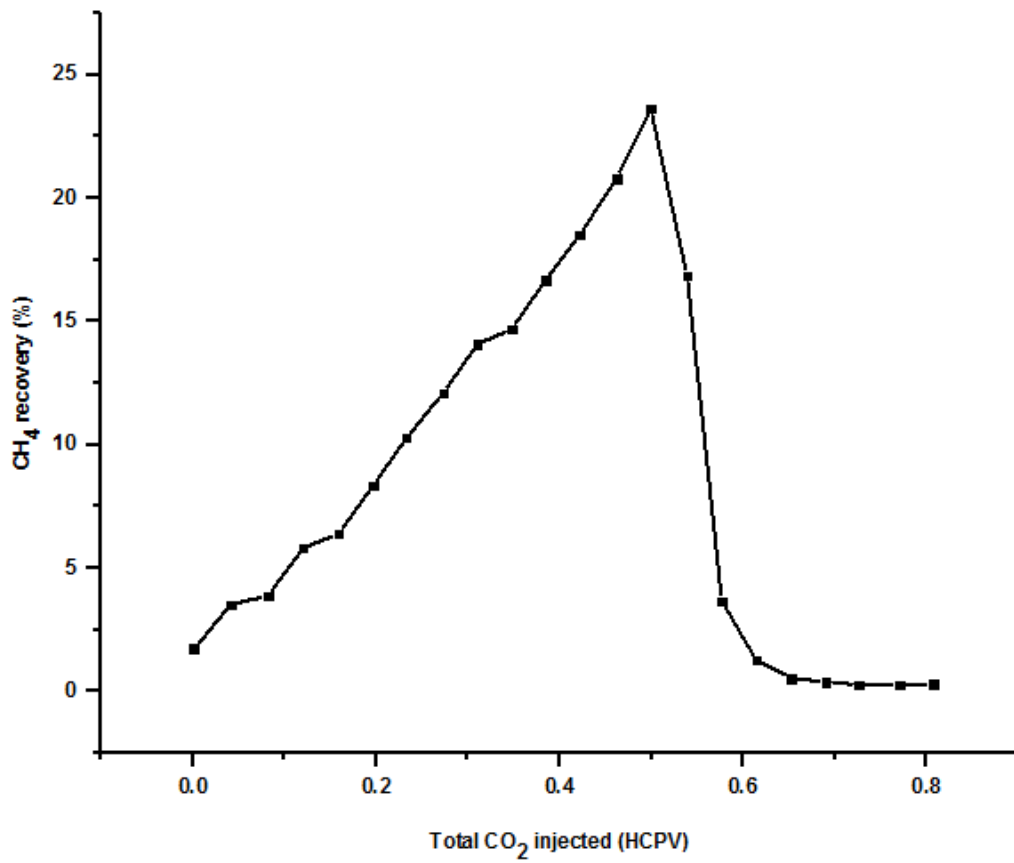**Fig. 7**. CH₄ recovery against HCPV of total CO₂ injected at 0.6ml

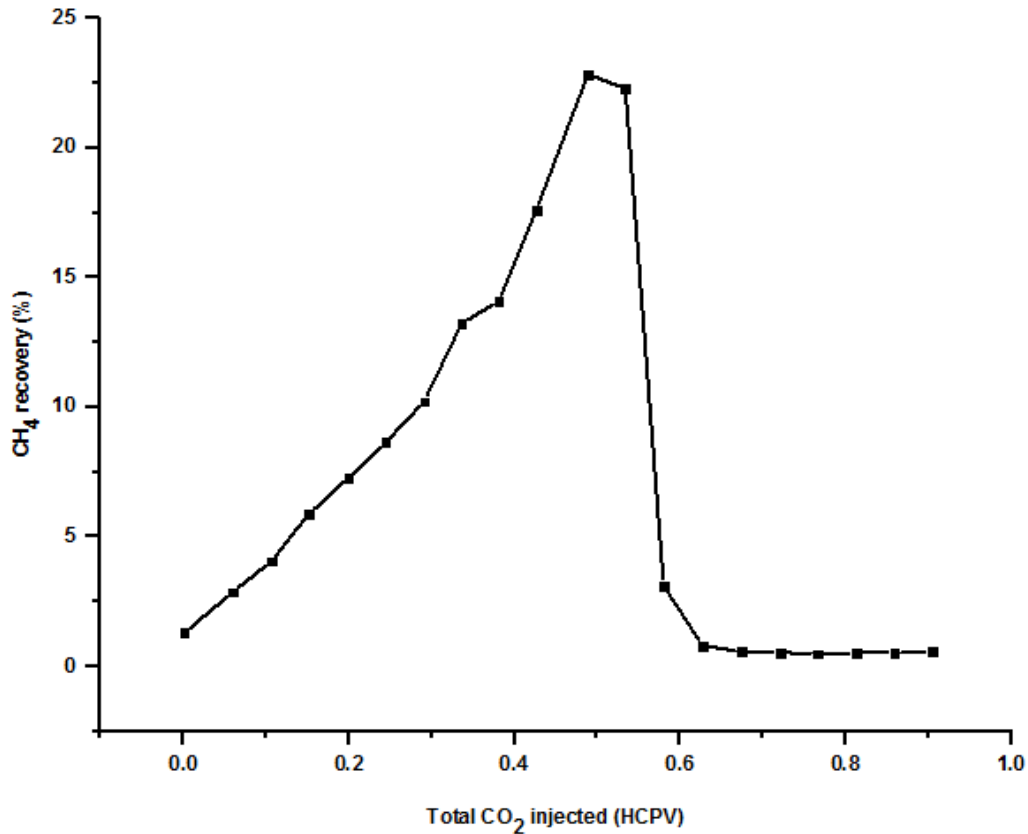**Fig. 8**. CH₄ recovery against HCPV of total CO₂ injected at 0.8ml

Fig. 9. CH_4 recovery against HCPV of total CO_2 injected at 1.0ml

4.2 Dispersion Coefficient and Dispersivity

The different injection rates were employed to determine the optimum injection rate from the range of interest. The compositions of CO_2 produced were used to evaluate the miscibility rate of CO_2-CH_4 interaction by adopting the longitudinal dispersion coefficient K_L as the fitting parameter. The values of the dispersion coefficients for different injection rates are shown in Table 2. The characteristics length scale of mixing (L) was adjusted in the OriginPro software regression tool to provide a better fit as advised by (Hughes et al., 2012; Liu et al., 2015; Abba et al., 2018), given that the interstitial velocity was kept unchanged for each run as assumed in the 1D advection-dispersion equation in Eqn. 2. As expected, the higher injection rates showed an early breakthrough in the CO_2; this agrees with the works reported by (Liu et al., 2015; Abba et al., 2018). Looking at Eqn. 5, It was evident that precise and reliable simulation of dispersion during enhanced recovery process requires a detailed understanding of molecular dispersion (D), tortuosity (τ), and dispersivity (α) at the condition relevant to natural gas displacement in porous media. The latest two parameters are properties of the porous medium (core sample) of which α can be determined from a set of experimental data in which the flow velocity through the medium is increasing at reasonable intervals like those described in this study. Although the pressure and temperature dependence of longitudinal dispersion coefficient (K_L) are acquired predominantly by that of D. Thus, accurate values of the molecular diffusion coefficient are prerequisites to a reliable dispersion correlation. Fuller, Schetter, and Gittings (1966) developed a numerical model through computer-aided correlation of 340 experimental points, expressed in Eqn. 7 was used to evaluate the molecular diffusion coefficient of CO_2-CH_4 at conditions relevant to enhanced gas recovery. The molecular diffusion coefficients, D, at experimental conditions of 1500 psig pressure and 40 °C temperature were evaluated. Using the measured grain diameter of 57.15µm reported by Abba et al. (2018) as the characteristic length scale of mixing, the medium *Peclet* numbers were evaluated using Eqn.4, taking (u) as the average interstitial velocity of the runs as an input variable. The P_{em} recorded were 0.02, 0.03, 0.03, 0.04, and 0.05. All values were < 0.1, which indicated the flow mechanism is dominated by diffusion within the entire experimental tests. Furthermore, the dispersivity (α) can be constructively determined by fixing Eqn.5 to the plots of

K_L/D against u/D, which is a straight line shown in Fig. 10. Considering the reports of (Coats, K.H & Whitson, 2004; Keith H. Coats et al., 2009; Honari et al., 2013; Hughes et al., 2012), they dispensed that the values of the dispersivity (α) in consolidated porous media are mostly smaller than 0.01 ft (0.003 m). Hughes et al. (2012) recorded dispersivity in a range of 0.0001 to 0.0011 m using Donnybrook core. Abba et al. (2018) reported 0.0006m of dispersivity and tortuosity of 29 in Bandera grey core plug with properties similar to those one used in this work. Generally, the longitudinal dispersion coefficient increases with an increase in flow velocity due to turbulence or eddy current development. The highest and least dispersion were recorded at maximum and minimum injection rates, as evident in Fig. 11 when the dispersion coefficients were plot against tests injection rates, invariably a linear relationship.

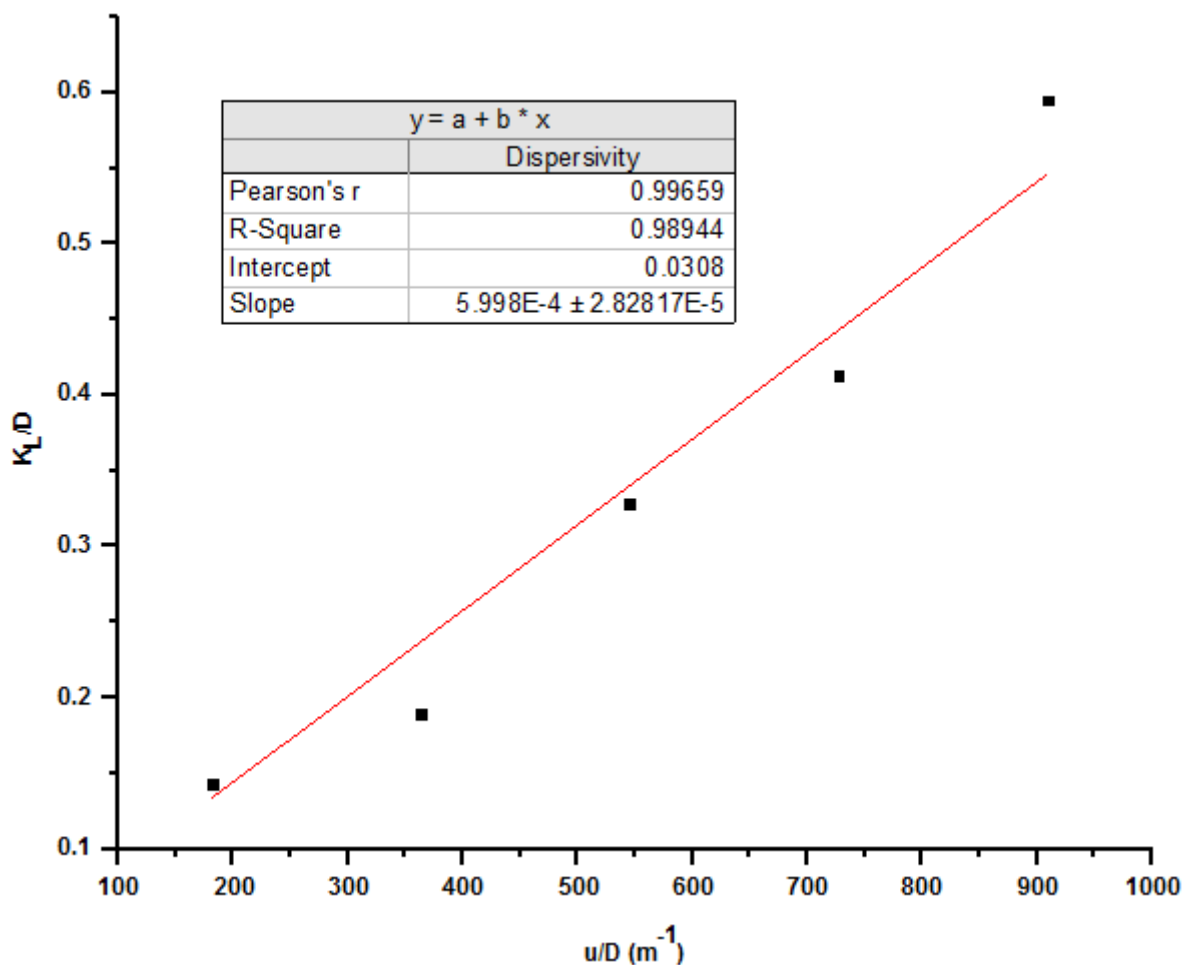| y = a + b * x	
	Dispersivity
Pearson's r	0.99659
R-Square	0.98944
Intercept	0.0308
Slope	5.998E-4 ± 2.82817E-5

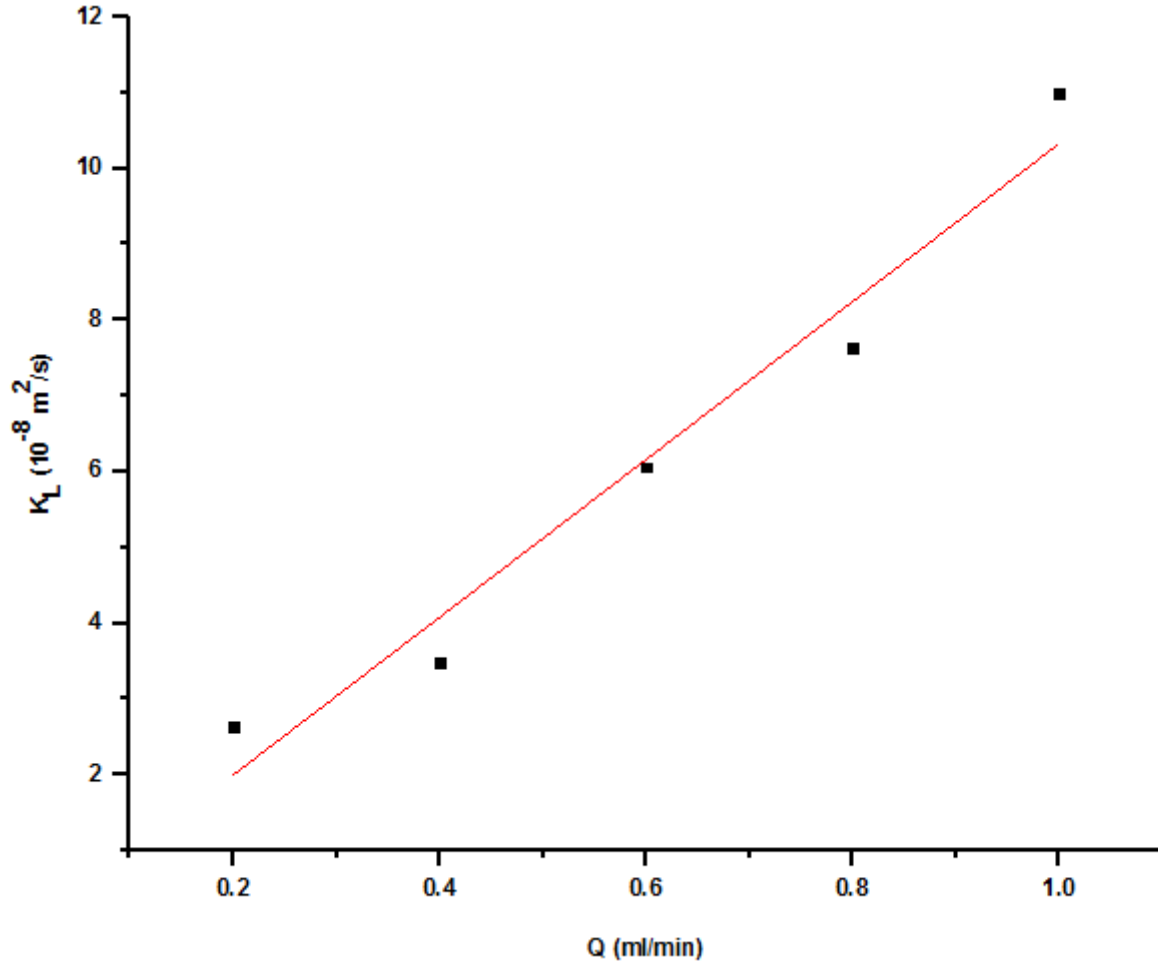Fig. 10. Plot of dispersion to diffusion coefficient ratio against interstitial velocity

Fig. 11. Plot of longitudinal dispersion coefficient ratio against injection rates

Injection at a low rate mainly results in more extended breakthrough (resident) time for gases in contact and increases the mixing of the gases yet again (Abba et al., 2018). This nascent mixing makes it challenging to use conventional CO_2 injection without an external factor to achieve higher CH_4 recovery and CO_2 storage at the same time. To curtail this problem, the inclusion of N_2 as a booster during CH_4 displacement by CO_2 injection was discussed in the next section. On this occasion, a 0.4 ml/min injection rate was employed for further CO_2 injection due to its significant combined CH_4 recovery and a substantial amount of injected CO_2 (HCPV) stored.

Table 2. Results summary for all the experimental runs at diffusion coefficient of 18.48 10^{-8} m²/s

Q (ml/min)	Interstitial Velocity (10^{-5} m/s)	Total CO_2 Injected (HCPV)	CO_2 Breakthrough (HCPV)	CO_2 Injected Stored (%)	CH_4 Recovery (%)	Dispersion Coefficient (10^{-8} m²/s)
0.2	3.36	0.36	0.20	35.62	59.63	2.64
0.4	6.72	0.37	0.22	58.03	39.97	3.49
0.6	10.08	0.56	0.33	56.82	26.61	6.06
0.8	13.44	0.81	0.54	66.10	24.59	7.63
1.0	16.80	0.90	0.53	68.51	27.74	10.99

4.3 Effect of N_2 as a booster gas during CO_2 flooding

The breakthrough indicates the first contact in which the injected gas species (CO_2 or N_2) came in contact with the displaced CH_4 gas along the core sample's length scale during the experiment. For conventional CO_2 flooding, the longer the breakthrough, the lower the sweep recovery efficiency due to the nascent mixing between the CO_2 and CH_4, as

evident with higher dispersion coefficients. This results in natural gas production with low calorific value and high purification cost, rendering the process uneconomical. In contrast, a delay in breakthrough was observed when N_2 was employed as a booster gas. Four sets of experiments were carried out at 1500 psig, 40 ^{0}C, and at varying booster gas volume of 0.06-0.29 HCPV. The variation in effluent compositions with total gas injection (HCPV) was monitored, as seen in Fig. 12. At the same time, Fig. 13 presented the effect of N_2 booster gas on CO_2 breakthrough compared to the conventional CO_2 injection at 0.4 ml/min. The CO_2 residence time was delayed for all the booster gas volumes employed. The injected amount of N_2 prior to the CO_2 injection exhibits a re-pressurization effect to produce maximum levels of CH_4 and a minimum fraction of CO_2 in the effluent stream of the core holder before CO_2 breakthrough due to its high conductivity. This affirmed the potential of N_2 for reservoir maintenance applications. The increase in booster gas volume was directly proportional to delayed CO_2 breakthrough, with the maximum at 30% (0.3) fraction of pore volume. The booster composition was monitored throughout the experiments from the GC machine. The higher the booster gas in the system, the more N_2 gas was recorded at the product stream, as seen in Fig. 15. This was a similar trend observed during the CO_2 flooding at higher injection rates. However, lower product contamination was recorded at lower booster gas volume with improved CH_4 recovery and CO_2 storage compared to that at 0.4ml/min optimum CO_2 flooding. This implies that injecting a small amount of N_2 before CO_2 injection in the reservoir promotes good CH_4 recovery and enables substantial volumes of CO_2 storage within the core plug's pore spaces. The introduction of N_2 displaces a larger amount of the CH_4 until it reached its breakthrough; this allows most of the CO_2 later injected to be trapped within the rock space without mixing with the nascent CH_4. More so, when the CO_2 reaches its breakthrough, a substantial clean volume of CH_4 has been recovered. The CO_2 find it difficult to disperse itself into the CH_4 in the presence of N_2, which acted as a barricade wall between the CO_2 and CH_4 interphase.

To optimize both CH_4 recovery and CO_2 storage, the fraction of the produced CO_2 and N_2 (X) at the exit stream must be minimized, while the change in the produced CO_2 fraction (ΔX) must be maximized. In so doing, the concentration profile curve can be flatting, invariably higher CH_4 recovery and CO_2 storage, as seen in Fig. 3. Natural gas products based on N_2 contaminants are more friendly than CO_2 based contaminants because most natural gas exploration fields accommodate higher nitrogen contamination than CO_2 based impurities. The sweetening process of CH_4-N_2 contamination is less expensive than CH_4-CO_2 due to the high compression energy cost and depressurizing process employed.
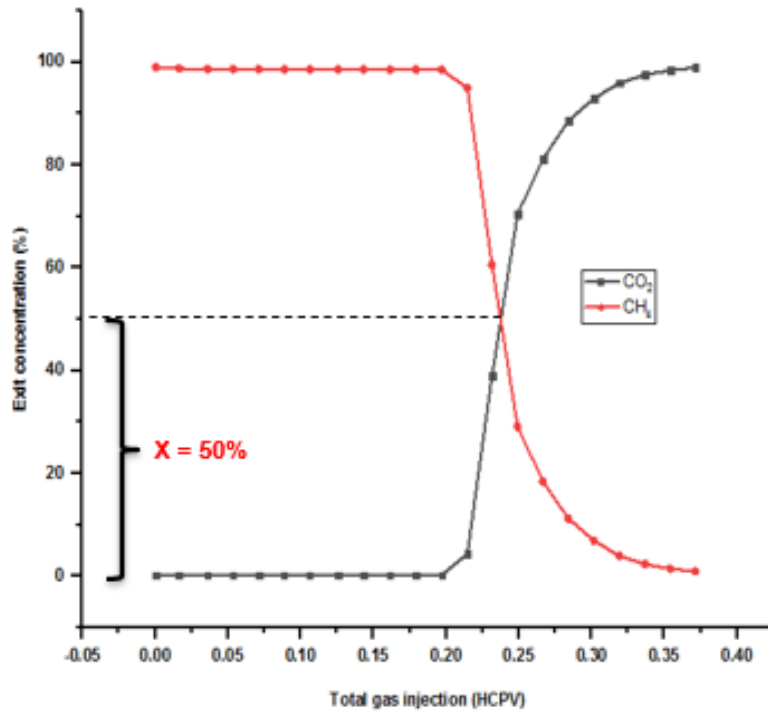
Fig. 12. Concentration profile at 0.4ml/min optimum conventional CO_2 injection
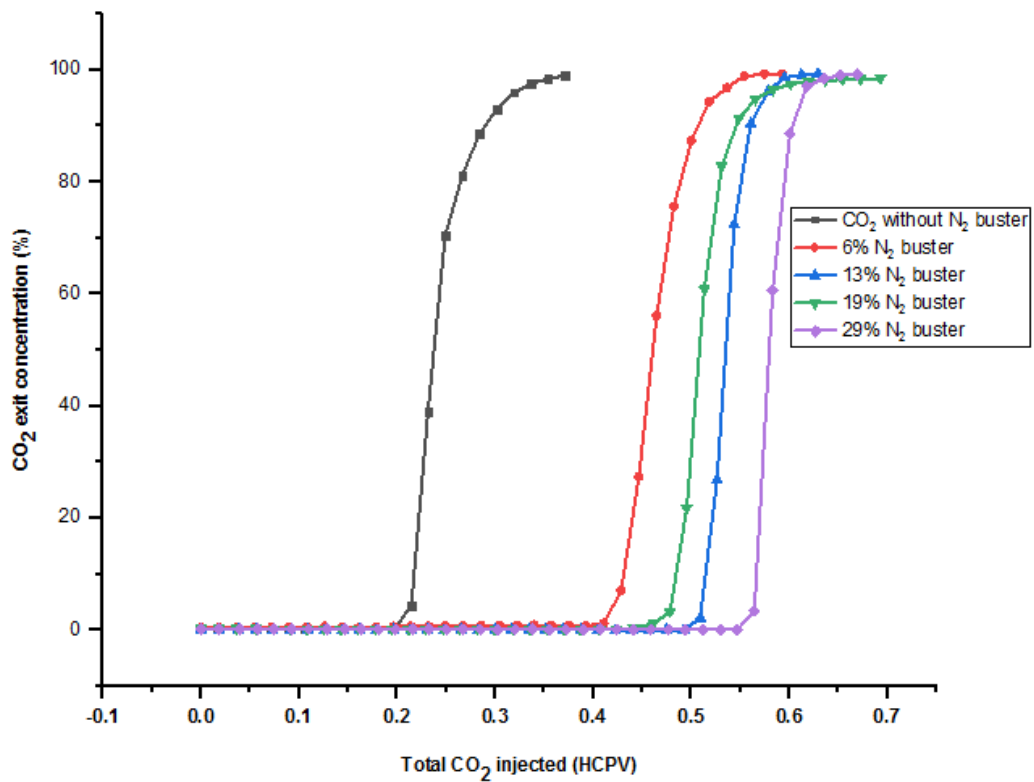

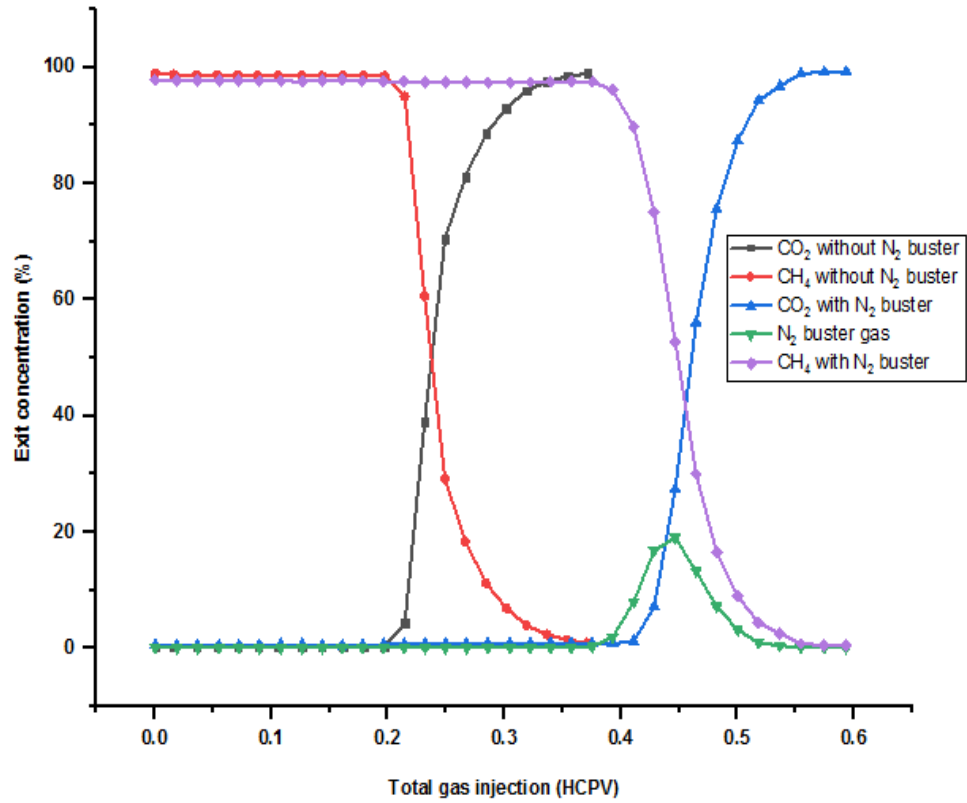**Fig. 13.** Effects of booster gas on CO_2 breakthroughs

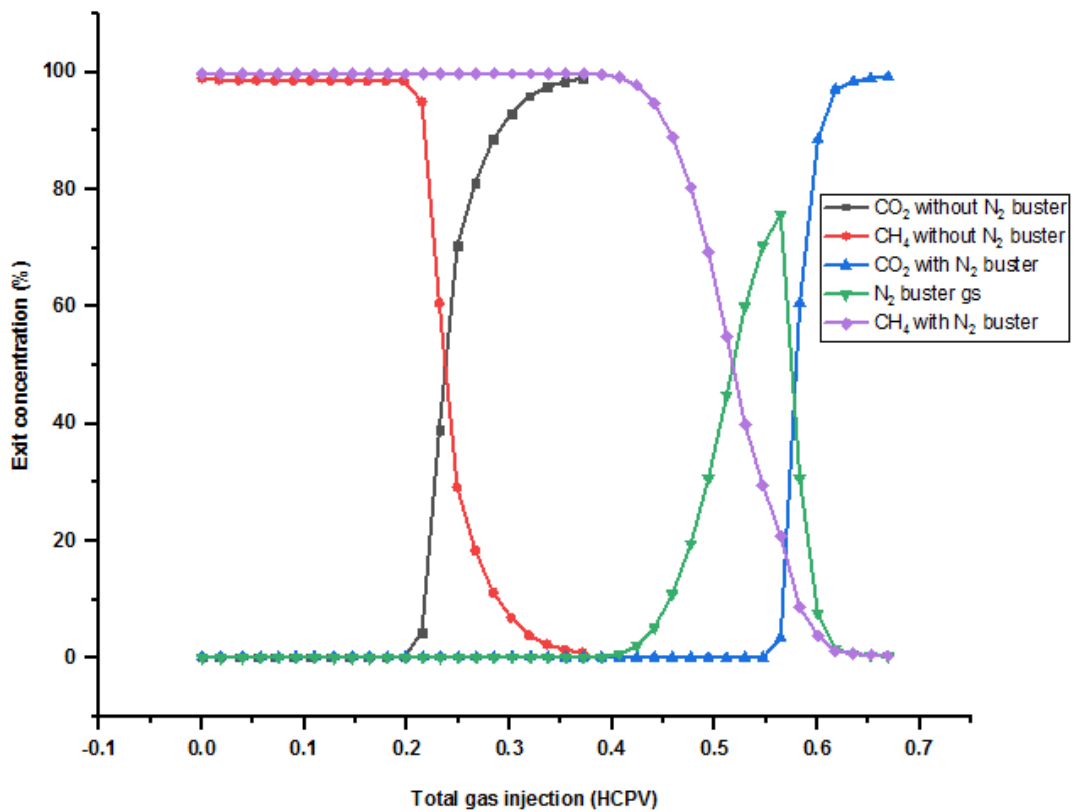**Fig. 14.** Concentration profile comparison at 6% booter gas

Fig. 15. Concentration profile comparison at 29% booster gas

More so, substantial CO_2 storage at the maximum booster amount was observed when a total fraction of 0.348 HCPV of CO_2 was injected. This was within the range of total CO_2 injected during 0.2 and 0.4 ml/min conventional CO_2

flooding. However, the later recorded high CO_2 storage than the latest 0.2 and 0.4ml/min injections. The excess amount of N_2 injected acted as a retardant, creating a thin barrier between the CO_2-CH_4 interface, promoting the CO_2 to descend for storage due to gravity. The produced CH_4 was grossly contaminated with the N_2 than CO_2, as seen from the N_2 and CO_2 intersecting the CH_4 curve in Fig. 15. Thus, the least recovery was recorded due to the excess amount of booster gas used. The reduction in the nascent CO_2-CH_4 mixing was achieved from the low dispersion coefficient value recorded. Furthermore, the experimental run at 0.06, 0.13, and 0.19 fraction of HCPV has a similar amount of total CO_2 injected with the 0.6ml/min conventional CO_2 flooding. The test at 0.13 HCPV of N_2 booster gave the highest CO_2 storage presented in Table 3. This value was characterised by the large differential pressure drop (dp) shown in Fig. 16. The highest recovery occurred when the least booster gas was used. This value was characterised by the least N_2 product contaminant and differential pressure (dp). However, it recorded the highest mole fraction of CO_2 produced, as presented in Fig. 14. Therefore, the presence of N_2 as a booster or impurity causes large changes in supercritical CO_2 behaviour as reported by (Xidong et al., 2019; Hughes et al., 2012; Janssen et al., 2018; Abba et al., 2018). To reduce gas separation cost, various authors proposed a longer residence (breakthrough) time should be considered for gas injection (Xiangchen et al., 2018) provided the excessive CO_2-CH_4 miscibility can be minimised. This will allow a large storage volume of CO_2 and, at the same time, recovered most of the residual natural gas. It worth noting that higher displacement efficiency is obtained at lower cushion volume.
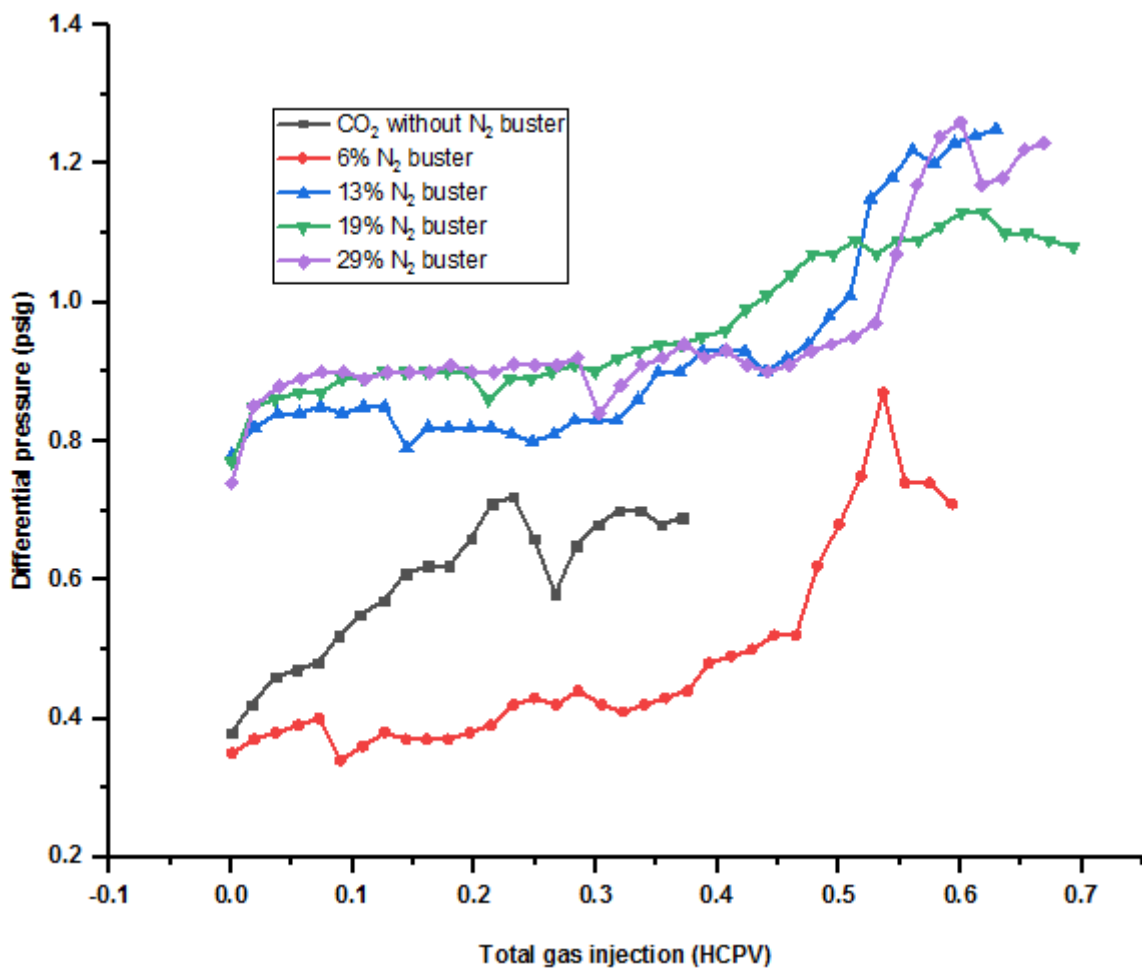

Fig. 16. A plot of differential pressure drops against experimental time with and without booster gas

Table 3. Results summary for all the experimental runs at diffusion coefficient of 18.48 10^{-8} m²/s

Case Study	Q (ml/min)	Interstitial Velocity (10^{-5} m/s)	CO_2 Injected (HCPV)	CO_2 Injected Stored (%)	CH_4 Recovery (%)	Dispersion Coefficient (10^{-8} m²/s)
Without N₂ booter						
	0.2	3.36	0.36	35.62	59.63	2.64
	0.4	6.72	0.37	58.03	39.97	3.49
	0.6	10.08	0.56	56.82	26.61	6.06
	0.8	13.44	0.81	66.10	24.59	7.63
	1.0	16.80	0.90	68.51	27.74	10.99
With N₂ booter						
(HCPV)						
	0.06	6.72	0.492	57.91	89.17	3.59
	0.13	6.72	0.486	68.67	64.81	2.78
	0.19	6.72	0.504	49.06	75.95	3.27
	0.29	6.72	0.348	63.47	44.39	2.59

5. Conclusions

A core flooding experiment was carried out to investigate the production of CH_4 during enhanced gas recovery displacement scenarios in N_2 as booster gas, to register the effects of its existence. CH_4 recovery was influenced by the inclusion of N_2 as booster gas before the CO_2 injection into the reservoir. The displacement efficiency of the current research exhibits improved results than the conventional CO_2 flooding. Overall, an improved CH_4 recovery, substantial CO_2 storage and less miscibility effect were noticed than conventional CO_2 flooding. The best-improved results occurred at the lower booster gas volumes with the optimum at 0.13 fraction of HCPV. This signifies the potential role of N_2 as a booster medium on CH_4 recovery and CO_2 storage. During the displacement process, the N_2 acts as a barrier wall, creating a thin film layer between CO_2 and CH_4, making it difficult for the CO_2 to penetrate and disperse into the CH_4 phase due to the blanketing effect of N_2 gas. This why a minimum length scale of mixing between displacing and displaced gases was achieved at 0.13 and 0.29 HCPV of booster gas. The critical temperature and pressure points of CO_2, N_2 and CH_4 are 31.05 and 1070, -146.9 and 492, -82.55 °C and 667 psig, respectively. Both nitrogen (N_2) and CO_2 can increase CH_4 recovery from oil and gas reservoirs. However, CO_2 drawbacks are mainly excessive mixing and high compression ratio, thus hindering the overall process non-economically viable.

In contrast, N_2 can be recovered virtually from the atmospheric air through air separation units. It requires less compression ratio than CO_2, so a lower amount of it is needed to create high pressure in the CH_4 reservoir. Further work will entail an examination of the effect of connate water salinity on this novel approach.

Nomenclature

|	
X	Mole fraction of injecting specie
ΔX	Change in mole fraction of injecting specie
S	Slope
C	Concentration
V_b	Bulk volume
S_{wi}	Water of saturation
$SiCO_2$	Supercritical carbon dioxide
HCPV	Hydrocarbon pore volume
D	Diffusion coefficient, m^2/s
Q	Flowrate, mil/min
t_D	Dimensionless time
x_D	Dimensionless distance
K_L	Longitudinal dispersion, m^2/s
k	Permeability, md
A	Cross section area, cm^2
L	Length of characteristic scale
dp	Differential pressure across the plug, atm
L_{exp}	Experimental length, m
μ	Viscosity, cP
P	Pressure, psig
T	Temperature, K
u	Interstitial velocity, m/s
ϕ	Core porosity, %
α	Dispersivity, m
τ	Tortuosity
P_e	Peclet number
P_{em}	Medium Peclet number
r	Radius of core sample, m

Appendix
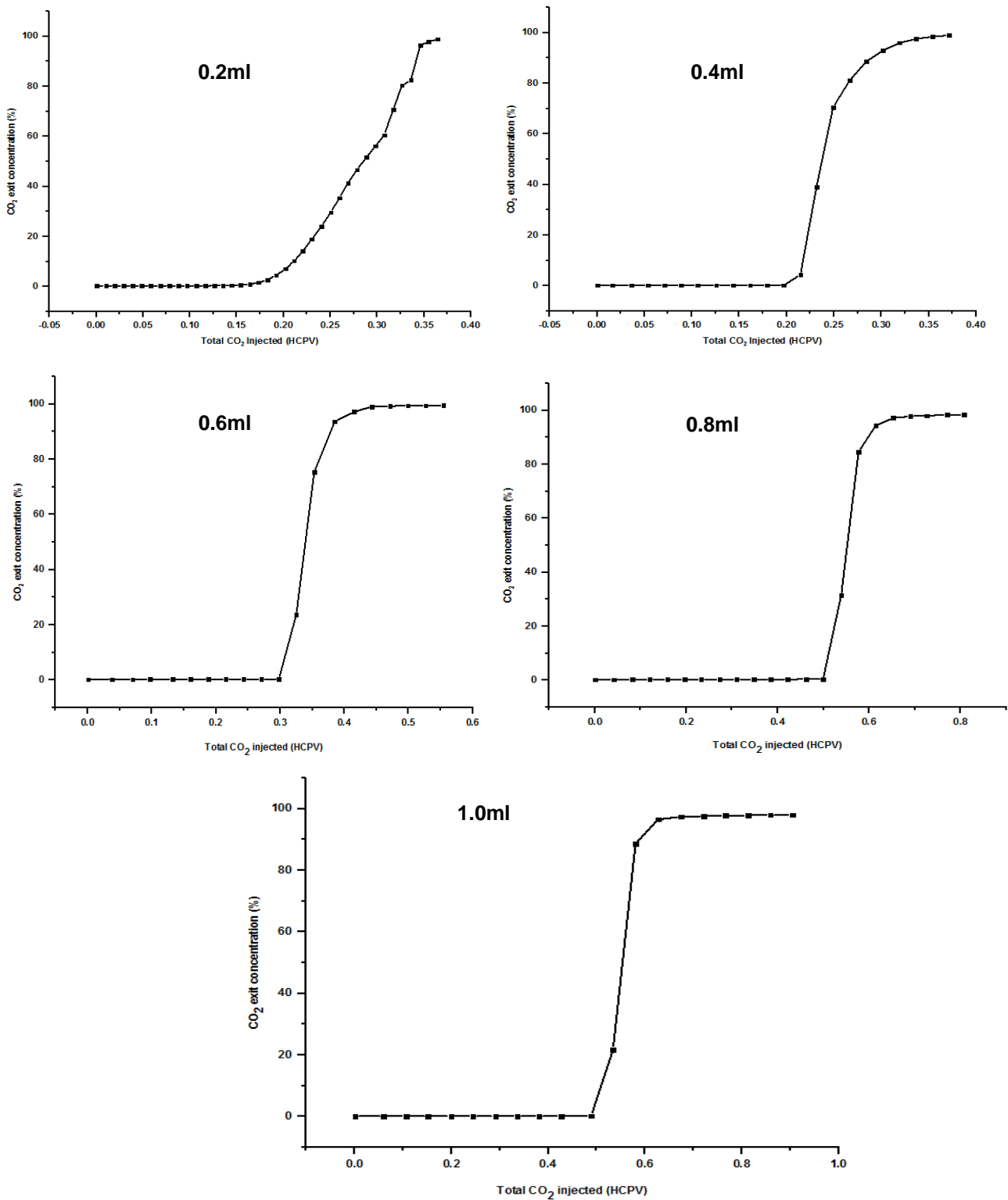
Fig. 17. CO_2 produced against HCPV of CO_2 injected at different injection rates of 0.2 – 1.0 ml/min
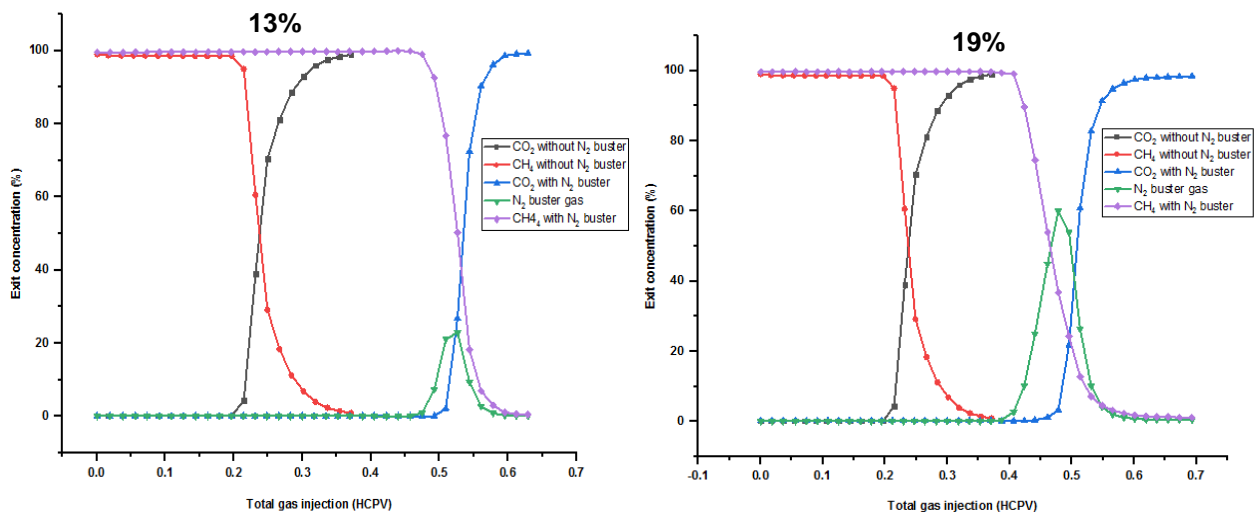
Fig. 18. Concentration profile comparison at 13 and 19% booster gas

References

Abba, M.K., Abbas, A.J., Athari, A., Mukhtar, A., & Nasr, G.G. (2018). Experimental Investigation on the Impact of Connate Water Salinity on Dispersion Coefficient in Consolidated Rocks Cores during EGR by CO_2 Injection. *Journal of Natural Gas Science and Engineering*, 60, 190-201. http://doi.org/10.1016/j.jngse.2018.10.007.

Abba, M.K., Abbas, A.J. & Nasr, G.G. (2017). Enhanced Gas Recovery by CO_2 Injection and Sequestration: Effect of Connate Water Salinity on Displacement Efficiency. SPE Abu Dhabi International Petroleum Exhibition & Conference. http://www.onepetro.org/doi/10.2118/188930-MS.

Al-abri, A., Sidiq H. & Amin R. (2009). Enhanced Natural Gas and Condensate Recovery by Injection of Pure $SCCO_2$, Pure CH_4 and Their Mixtures: Experimental Investigation. SPE Annual Technical Conference and Exhibition, New Orleans, Lousiana, USA, 4-7 October, 1-13.

Al-Hasami A, Ren Shaoran, Tohidi. CO2 injection for enhanced gas recovery and geo-storage: Reservoir simulation and economics. In: SPE EUROPEC/EAGE annual conference, 13e16 June; 2005. Madrid, Spain, http://dx.doi.org/10.2118/94129-MS.

Anonymous, 2020. NiGen Annual Report, 2020: https://nigen.com/nitrogen-injection-enhanced-oil-recovery-techniques-eor/

Coats, K.H., Whitson, C.H., Thomas, K. (2009). Modelling conformance as dispersion. SPE Reservoir Eval. Eng. 12, 33–47. https://doi.org/10.2118/90390-PA.

Coats, K. H., & Whitson, C. H. (2004). SPE 90390 Modelling Conformance as Dispersion.

Fuller, E. N., Schettler, P. D., and Giddings, J. C. (1966). New method for prediction of binary gas-'phase diffusion coefficients, Ind. Eng. Chem., 58, 18–27.

Honari, A., Bijeljic, B., Johns, M. L., & May, E. F. (2015). Enhanced gas recovery with {CO_2} sequestration: The effect of medium heterogeneity on the dispersion of supercritical CO_2–CH_4. *International Journal of Greenhouse Gas Control*, *39*(0), 39–50. http://doi.org/http://dx.doi.org/10.1016/j.ijggc.2015.04.014

Honari, A., Hughes, T. J., Fridjonsson, E. O., Johns, M. L., & May, E. F. (2013). Dispersion of supercritical CO_2 and CH_4 in consolidated porous media for enhanced gas recovery simulations. http://doi.org/10.1016/j.ijggc.2013.08.016

Honari, A., Zecca, M., Vogt, S. J., Iglauer, S., Bijeljic, B., Johns, M. L., & May, E. F. (2016). The impact of residual water on CH_4-CO_2 dispersion in consolidated rock cores. http://doi.org/10.1016/j.ijggc.2016.04.004

Hughes, T. J., Honari, A., Graham, B. F., Chauhan, A. S., Johns, M. L., & May, E. F. (2012). CO_2 sequestration for enhanced gas recovery: New measurements of supercritical CO_2–CH_4 dispersion in porous media and a

review of recent research. *International Journal of Greenhouse Gas Control*, *9*, 457–468. http://doi.org/10.1016/j.ijggc.2012.05.011

Huysmans, M., & Dassargues, A. (2005). Review of the use of Peclet numbers to determine the relative importance of advection and diffusion in low permeability environments. *Hydrogeology Journal*, *13*(5–6), 895–904. http://doi.org/10.1007/s10040-004-0387-4

Janssen, M. T. G., Azimi, F., Zitha, P. L. J. (2018). Immiscible Nitrogen Flooding in Bentheimer Sandstones: Comparing Gas Injection Schemes for Enhanced Oil Recovery. Society of Petroleum Engineers. Available at: doi:10.2118/190285-MS

Keith D. W. (2009). Science, 325, 1654–1655.

Khan, C., Amin R. & Madden G. (2013). Carbon dioxide injection for enhanced gas recovery and storage (reservoir simulation). *Egyptian Journal of Petroleum*, 22(2), 225-240. http://www.sciencedirect.com/science/ article/pii/S1110062113000500.

Li, M., Vogt, S., May, E. and Johns, M., 2019. In Situ CH_4–CO_2 Dispersion Measurements in Rock Cores. *Transport in Porous Media*, 129(1), pp.75-92.

Liu, S., Zhang, Y., Xing, W., Jian, W., Liu, Z., Li, T., & Song, Y. (2015). Laboratory experiment of CO_2-CH_4 displacement and dispersion in sandpacks in enhanced gas recovery. *Journal of Natural Gas Science and Engineering*, *26*, 1585–1594. http://doi.org/10.1016/j.jngse.2015.04.021

Mamora, D.D., Seo, J.G., 2002. Enhanced recovery by carbon dioxide sequestration in depleted gas reservoirs. SPE Annu. Tech. Conf. Exhib. 1–9.

Meehl G. A., Washington W. M., Collins W. D., Arblaster J. M., Hu A., Buja L. E., Strand W. G., Teng H. (2005). S cience, 307, 1769–1772.

Newberg, M.., & Foh, S., 1988. Measurement of Longitudinal Dispersion Coefficients for Gas Flowing Through Porous Media. *SPE*, 5–9.

Nuhu Mohammed, Abubakar J. Abbas, Godpower C. Enyi, Donatus E. Edem, Salihu M. Suleiman (2020). "Enhanced Gas Recovery by Nitrogen Injection: The effects of injection velocity during natural gas displacement in consolidated rocks", Journal of Natural Gas Science and Engineering,83,1-14. https://doi.org/10.1016/j.jngse.2020.103513

Oldenburg, C.M. & Benson S.M., 2002. CO_2 Injection for Enhanced Gas Production and Carbon Sequestration. SPE International Petroleum Conference and Exhibition in Mexico. http://www.onepetro.org/ doi/10.2118/74367-MS.

Oldenburg, C. M. (2001). Pruess, K. *EOS7C: Gas reservoir simulation for TOUGH2*; Lawrence Berkeley National Laboratory Report: 2 in preparation.

Perkins, T.., & Johnston, O. (1963). A Review of Diffusion and Dispersion in Porous Media. *Society of Petroleum Engineers Journal*, 3(01), 70–84. 10.2118/480-PA

Patel, M. J., May, E. F., & Johns, M. L. (2016). High-fidelity reservoir simulations of enhanced gas recovery with supercritical CO_2. *Energy*, *IN PRESS*, 548–559. http://doi.org/10.1016/j.energy.2016.04.120

Pooladi-Darvish, M., Hong, H., Theys, S., Stocker, R., Bachu, S., & Dashtgard, S. (2008). CO_2 injection for enhanced gas recovery and geological storage of CO_2 in the Long Coulee Glauconite F Pool, Alberta. *Proceedings - SPE Annual Technical Conference and Exhibition*, 4, 2271–2281. http://doi.org/10.2118/115789-MS

Shabani, B., Vilcáez, J., 2017. Prediction of CO_2-CH_4-H_2S-N_2 gas mixtures solubility in brine using a non-iterative fugacity-activity model relevant to CO_2-MEOR. J. Petrol. Sci. Eng. 150, 162–179. https://doi.org/10.1016/j.petrol.2016.12.012.

Shtepani, E. (2006). CO_2 sequestration in depleted gas/condensate reservoirs.

Sidiq, H., Amin, R., der Steen, E. Van, & Kennaird, T. (2011a). Super critical CO2-methane relative permeability investigation. *Journal of Petroleum Science and Engineering*, *78*(3–4),654–663. http://doi.org/10.1016/j.petrol.2011.08.018

Sim, S. S. K., Brunelle, P., Canada, Q., Systems, F., Turta, A. T., & Singhal, A. K. (2008). SPE 113468 Enhanced Gas Recovery and CO_2 Sequestration by Injection of Exhaust Gases from Combustion of Bitumen. *Journal of Changes*, (1), 1–10.

Sim, S. S. K., Turta, A. T., Singhal, A. K., & Hawkins, B. F. (2009). Enhanced gas recovery: Factors affecting gas-gas displacement efficiency. *Journal of Canadian Petroleum Technology*, *48*(8), 49–55. http://doi.org/10.2118/09-08-49

Sim, S., Turta, A. T., Singhal, A., & Hawkins, B. F. (2009). Enhanced Gas Recovery: Effect of Reservoir Heterogeneity on Gas-Gas Displacement. *Candian International Petroleum Conference*, (June), 1–14. http://doi.org/10.2118/2009-023

Stolaroff J. K., Keith D. W., Lowry G. V. (2008). Environmental Science Technology, 42, 2728–2735.

Turta, A. T., Sim, S. S. K., Singhal, A. K., & Hawkins, B. F. (2007). Basic Investigations on Enhanced Gas Recovery by Gas-Gas Displacement.

Turta, A.T., S.S.K. Sim, A.K. Singhal, B.F. Hawkins (2009). Enhanced Gas Recovery: Factors Affecting Gas-Gas Displacement Efficiency. *Journal of Canadian Petroleum Technology,* 48(08), 1- 12.

Takahashi, S., Iwasaki, H., 1970. The diffusion of gases at high pressures. III. The diffusion of CO_2, in the CO_2–CH_4 system. Bulletin of the Chemical Research Institute of Non- Aqueous Solutions, Tohoku University 20, 27–36.

Wang, T., et al., 2018. Molecular simulation of CO_2/CH_4 competitive adsorption on shale kerogen for CO_2 sequestration and enhanced gas recovery. J. Phys. Chem. C 122 (30), 17009–17018. https://doi.org/10.1021/acs.jpcc.8b02061.

Xidong Du, Min Gu, Zhenjian Liu, Yuan Zhao, Fulong Sun, and Tengfei Wu, 2019. Enhanced Shale Gas Recovery by the Injections of CO_2, N_2, and CO_2/N_2 Mixture Gases. *Journal of energy and fuels*. DOI: 10.1021/acs.energyfuels.9b00822

Yu, D., Jackson, K., & Harmon, T. C. (1999). Dispersion and diffusion in porous media under supercritical conditions. *Chemical Engineering Science*, *54*(3), 357–367. http://doi.org/10.1016/S0009-2509(98)00271-1

Zhang, Y., Liu, S., Song, Y., Zhao, J., Tang, L., Xing, W., Jian, W., Liu, Z., Zhan, Y. (2014). Experimental investigation of CO_2-CH_4 displacement and dispersion in sand pack for enhanced gas recovery. *Energy Procedia*, 61, 393-397. http://dx.doi.org/10.1016/j.egypro.2014.11.1133.

Ziabakhsh-Ganji, Z., Kooi, H., 2012. An Equation of State for thermodynamic equilibrium of gas mixtures and brines to allow simulation of the effects of impurities in subsurface CO_2 storage. Int. J. Greenh. Gas Control 11, 21–34. https://doi.org/10.1016/ j. ijggc.2012.07.025.